

Intrabiliary MRI-monitored Local Delivery of Motexafin Gadolinium

Feng Zhang¹, Yanfeng Meng¹, Stephanie Soriano¹, Patrick Willis¹, David Glickerman¹, and Xiaoming Yang¹
¹Radiology, University of Washington, Seattle, Washington, United States

PURPOSES: Pancreatobiliary malignancy with biliary obstruction has a very poor prognosis. Insufficient therapeutic agent delivery to the tumor is one of the main contributors to chemoresistance in pancreatobiliary cancers. Intrabiliary local delivery of high dose therapeutic agents into bile duct walls may overcome this problem. The aim of this study was to develop a new technique of using intrabiliary MRI to monitor local delivery of a multifunctional agent, motexafin gadolinium (MGd, Pharmacyclics Inc.), into pig common bile duct (CBD) walls.

METHODS: An *in vivo* study was performed on 6 pigs. Laparotomy was performed to expose the gallbladder. Under X-ray fluoroscopy, via a transcholecystic access, a microporous balloon and a 0.032-inch MR imaging guidewire (MRIG) were placed into the CBD (Figure 1). After closure of the abdominal incision, pigs were transferred for MR imaging. We acquired two sets of fat-suppressed and respiration-gated T1 weighted images using a Torso phase-array surface coil and the MR imaging-guidewire, pre- and post- intrabiliary MGd delivery. A mixture of MGd (75 μ g/mL) and trypan blue dye was infused into the CBD wall at 0.5mL/sec through a microporous balloon. MR imaging was performed with a turbo field echo sequence (TFE) using 10/1-msec TR/TE, 300-mm FOV, 15° flip angle, 5-mm slice thickness, 320 \times 320 matrix, and 5 NEX. We measured signal intensities (SI) of the CBD walls (SI_{CBD}) and the peri-CBD tissues ($SI_{peri-CBD}$) using four ROIs along the CBDs at 0, 3, 6, and 9 o'clock, and then calculated the average contrast-to-noise ratio (CNR) using $(SI_{CBD} - SI_{peri-CBD}) / \text{standard deviation of the background noise (SD}_{noise})$. Immediately after MR imaging, the MGd/blue-infused CBD segment or un-infused CBD segment (as a control) was harvested for histologic correlation to confirm the successful penetration of MGd/trypan blue into the CBD wall. We cryosectioned the CBDs at 8 μ m, and then examined the histologic slides by using (i) laser confocal microscopy to detect red-fluorescent MGd and (ii) light microscopy to detect blue dye infiltration in the CBD walls. We used a paired Student *t*-test to compare the average CNRs of CBDs between (a) the images taken before and after infusion of MGd/blue mixture; and (b) images taken using the surface coil and the intrabiliary MR imaging-guidewire. A *P* value less than 0.05 was considered statistically significant.

RESULTS: Figure 2 summarizes the average CNRs obtained from both pre-MGd/blue-infusion MR images and post-MGd/blue-infusion MR images using either a surface coil or an intrabiliary MR imaging-guidewire. Post-MGd/blue-infusion MRI demonstrated a higher average CNR than pre-MGd/blue-infusion MRI when using either the surface coil (11.6 \pm 4.2 VS 5.7 \pm 2.8, *P*=0.025) or the intrabiliary MR imaging-guidewire (41.5 \pm 9.7 VS 29.6 \pm 6.3, *P*=0.046). Intrabiliary MRI generated a higher average CNR than surface coil-based MRI, on both pre-infusion images and post-infusion images (*P*=0.003 and 0.005). Histological examination confirmed these MRI findings, demonstrating as blue dye infiltration and MGd-emitting fluorescence within the CBDs (Figure 3).

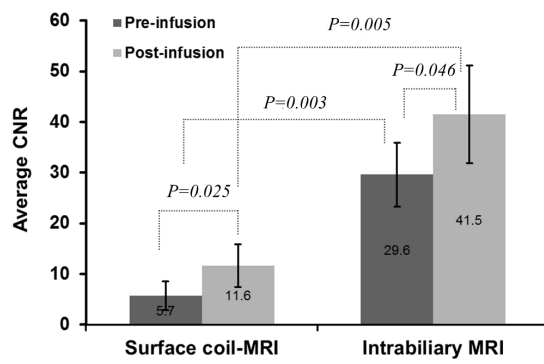


Fig.2. Average CNRs of CBDs of living pigs. CNRs are higher for post-MGd/blue infusion than pre-MGd/blue infusion, and higher for intrabiliary MRI than surface coil-based MRI.

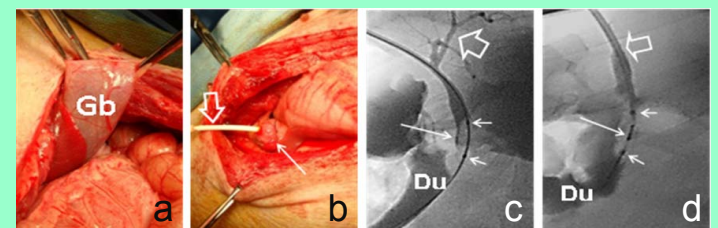


Fig.1. Surgery and cholangiography of the intrabiliary interventional procedure. (a&b) Via the laparotomy, the gallbladder (Gb) is exposed. (b) Transcholecystic insertion of a 6F introducer (open arrow) into the CBD. The long arrow indicates the gallbladder. (c) X-ray cholangiography shows the saline-inflated balloon (long arrow) as a filling defect on the cholangiogram with the contrast agent outlining the left hepatic duct (open arrow). Two short arrows indicate the two metal markers of the balloon. Du = duodenum. (d) The MR imaging-guidewire (long arrow) is advanced via the introducer (open arrow) into the inflated balloon catheter. Two short arrows indicate the two metal markers of the balloon.

We cryosectioned the CBDs at 8 μ m, and then examined the histologic slides by using (i) laser confocal microscopy to detect red-fluorescent MGd and (ii) light microscopy to detect blue dye infiltration in the CBD walls. We used a paired Student *t*-test to compare the average CNRs of CBDs between (a) the images taken before and after infusion of MGd/blue mixture; and (b) images taken using the surface coil and the intrabiliary MR imaging-guidewire. A *P* value less than 0.05 was considered statistically significant.

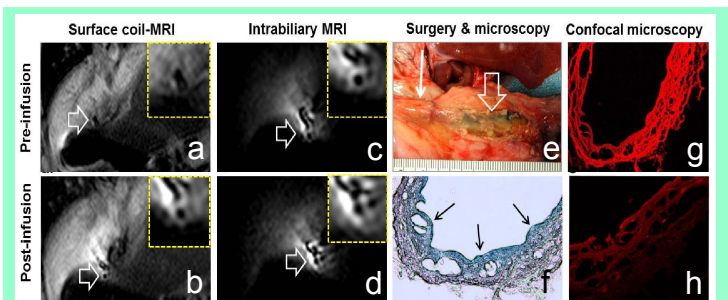


Fig.3. MRI-monitored local MGd/blue delivery into the CBD wall with a surface coil (a&b) and an intrabiliary MRIG (c&d), demonstrating MGd-enhanced CBD region (arrows on b&d) after intrabiliary MGd/blue infusion. Insets represent the magnifications of the CBD regions. (e) Surgery shows blue-stained CBD (open arrow), which is confirmed by histologic correlation as blue-penetrated CBD wall (arrows on f). The long arrow on (e) indicates the control CBD segment with no MGd/blue infusion. (g) Confocal microscopic imaging shows MGd-created red fluorescence in the CBD wall, compared to the control CBD segment with no MGd/blue infusion, in which only autofluorescence is seen (h).

CONCLUSIONS: This study demonstrates the feasibility of using MRI to monitor the intrabiliary local delivery of MGd into CBD walls, which may open new avenues to effectively manage obstructive pancreatobiliary malignancies.